Estimation of Strong Ground Motion in the 1995 Kobe Earthquake based on Building Damage Data

by

Naoya Yamaguchi* and Fumio Yamazaki**

ABSTRACT

The 1995 Kobe Earthquake caused unprecedented building damage in the Hanshin-Awaji area. In order to evaluate the building damage in this area due to the earthquake, it is important to estimate the distribution of earthquake ground motion. However, since the number of strong ground motion records is not enough in the heavily damaged area, it is necessary to estimate the distribution using other data sources. In this study, the fragility curves for residential buildings were constructed using the building damage data from the field survey by the AIJ and CPIJ group and the recorded motions. The fragility curves obtained were then employed to estimate ground motion distribution in the district level for the Kobe and its surrounding areas during the 1995 Kobe Earthquake

INTRODUCTION

The Kobe (Hyogoken-Nanbu) Earthquake directly struck the densely populated Kobe and its neighboring cities in the early morning of January 17, 1995 and caused huge direct losses to infrastructures and private properties. In order to evaluate the building damage in this area due to the earthquake, it is important to estimate the distribution of earthquake ground motion. In the earthquake, scores of strong ground motion records were obtained in the heavily damaged area by several organizations. However, since they are still not enough in number for estimating the detailed spatial distribution of ground motion during the event, it is necessary to estimate the distribution using other data sources.

The estimation of the distribution of earthquake ground motion in the affected area due to the Kobe Earthquake have been conducted by several researches. Midorikawa et al. (1996) estimated the distribution of the peak ground velocity (PGV) in Kobe and its neighboring cities using the overturning ratio of tombstones. Hayashi et al. (1997a, 1997b) and Miyakoshi et al. (1998) estimated the distribution of PGV in the damaged area using the damage ratio of buildings in the district level.

In this study, as well, the relationships between the building damage and the ground motion indices are constructed. As the strong motion indices, the peak ground acceleration (PGA), PGV, the spectrum intensity (SI), and the instrumental JMA (Japan Meteorological Agency) intensity are considered. The fragility curves obtained for the residential buildings in the atfected area are then employed to estimate the strong motion distributions in the 1995 Kobe Earthquake.

* Graduate Student, Department of Civil Engineering, The University of Tokyo, Japan.

** Associate Professor, Institute of Industrial Science, The University of Tokyo, Japan.

FRAGILITY CURVES OF RESIDENTIAL BUILDINGS

Ground Motion and Building Damage Data

In the Kobe Earthquake, scores of strong ground motion records were obtained by the Committee of Earthquake Observation and Research in the Kansai Area (CEORKA), JMA, the Ministry of Construction, the Ministry of Transport, Japan Railway group, Osaka Gas Company, Kansai Electric Power Company and so on (Ejiri et al., 1996). In this study, among them, free field records were used as the ground motion indices to construct fragility curves. Those records include restored clipped records (Kagawa et al., 1996).

Several building damage surveys were conducted by groups of researches and engineers after the Kobe Earthquake. In this paper, ground motion distributions are estimated by using building damage data. So, it is necessary to use the result of the damage survey which was carried out based on the same standard throughout the stricken area. The Building Research Institute (BRI, 1996), the Ministry of Construction, digitized the results of the damage survey conducted by a group of the Architectural Institute of Japan (AIJ), the City Planning Institute of Japan (CPIJ) and Hyogo Prefectural Government (AIJ & CPIJ, 1995). Since this survey was conducted throughout the stricken area with the same damage criteria, in this study, fragility curves are created by using the building damage data compiled by the BRI. The damage level of the BRI data is classified into four levels: "heavy", "moderate", "insignificant", "no damage". Note that this classification is similar to the damage state classification of ATC-38 (Shinozuka et al., 1997). In addition to the BRI's building damage data, the results of building damage surveys by local governments (Osaka City Fire Department, 1996; Osaka Prefecture, 1997) are also used to reflect the ground motion indices in the slightly damaged area to fragility curves.

Relationships between Earthquake Ground Motion and Building Damage

In this paper, 17 recorded free field motions were used. Figure 1 shows the observation points of strong ground motion included within the area to estimate ground motion distributions in this study. Those points include the ones which were not used in this research. The reasons are that the records were not free field ones or that the number of the BRI's building damage data around the observation point was not enough.

In order to construct fragility curves for buildings, the building damage ratio around each observation point was calculated. The method of selecting the area represented by each seismometer is as follows. In case of using the BRI's building damage data, the district block (corresponding to the postal address) where a reference seismometer is placed and its surrounding blocks were selected for the corresponding area of the seismometer. In selecting the surrounding blocks, the extent of damage and the subsurface soil were considered: only the blocks with the similar condition as the reference block were selected. Figure 2 shows an example of the selection of the area represented by a seismometer. In case of JMA Kobe Station, because there are more than 300 residential buildings in the district block and the block's ground condition is different from the surrounding blocks, only one block is selected for the corresponding area of the seismometer. In case of Fukiai Gas Supply Station, there are few data of residential buildings in the reference block and the block's subsurface soil condition is similar to the surrounding blocks. Therefore, the reference block and the surrounding ones are selected. In case of using local governments' data, the city or the ward (for Osaka City) where a reference seismometer is located was selected for the corresponding area represented by the seismometer.

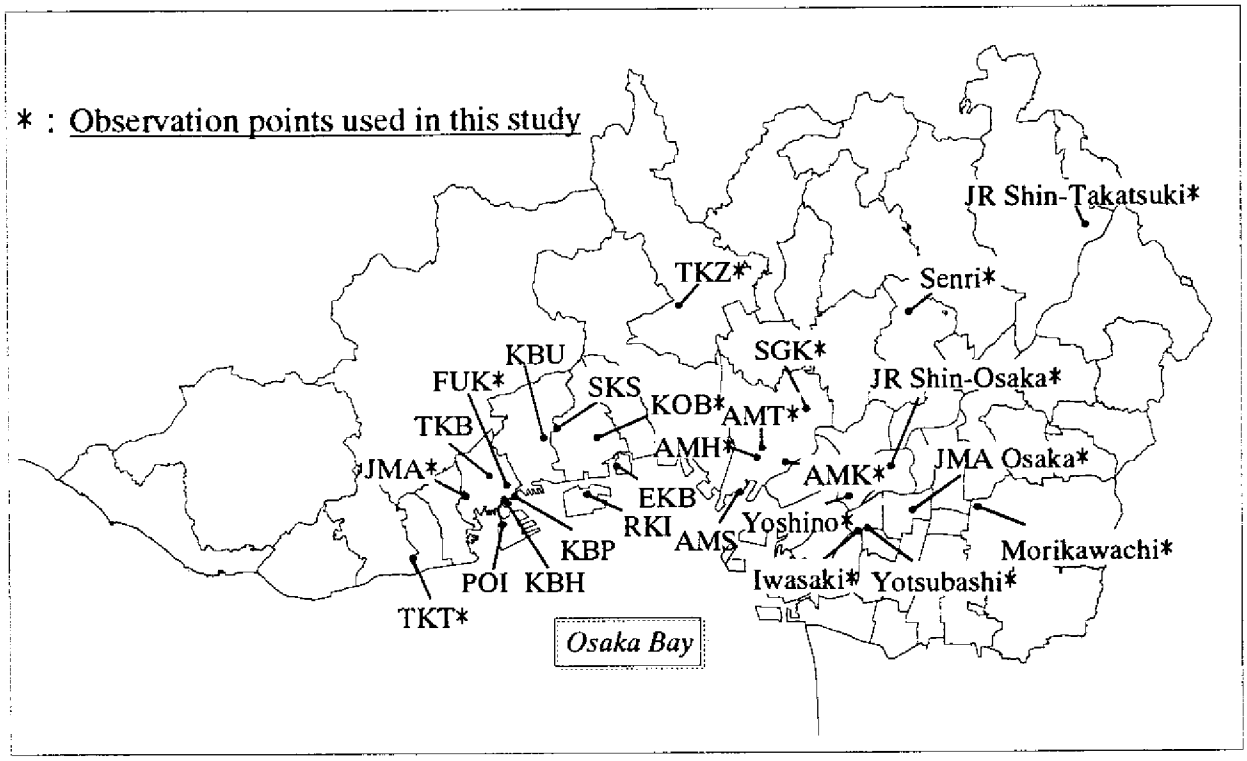

Fig. 1 Location of recorded motions used in this study

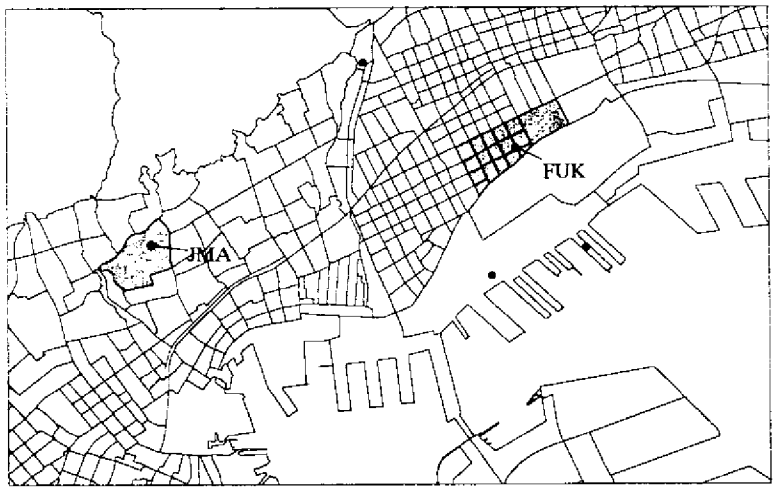

Fig. 2 Example of the selection of the areas represented by seismometers

The building damage ratios for the areas corresponding to the 17 seismometers were calculated. In calculating the damage ratio of buildings represented by a seismometer, we should better select buildings with similar fragility characteristics. The BRI data are classified by the number of stories and the use of buildings, and have no information on the structural type. Note that the structural type, e.g. wood-frame, reinforced concrete (RC), steel (S), is highly related to the fragility of buildings. It is also noted that the number of wood-frame buildings is largest for most areas and most of one or two storied residential

buildings are made of wood-frame in Japan. Considering these facts, the low-storied (one to two-storied) residential buildings in the BRI data were considered mostly as wood-frame buildings and hence, the damage ratio for the low-storied residential buildings were assumed to give the damage ratio for wood-frame buildings. Using the BRI data represented by the seismometers, the ratio of buildings with "heavy damage" (R_h), the ratio equal or more than "moderate damage" (R_m) and the ratio equal or more than "insignificant damage" (R_l) were calculated.

For the areas using the local government data, because the building damage criteria were different from the BRI data (Murao et al., 1998), the damage ratios calculated from the local government data should be converted. Since the earthquake ground motion was rather small in those areas, all the damaged buildings were assumed to be wood-frame (Note that "wood-frame" buildings have smallest seismic resistance in general). The total number of wood-frame buildings in a city or a ward was estimated by the total number of buildings in the region (Statistics Bureau, Management and Coordination Agency, 1995) multiplied by the ratio of residential buildings for all the BRI data. The damage ratio of wood-frame buildings in the region was then calculated employing these assumptions. Similar as for the BRI data, the ratio of "heavy damage" (R^*_h) and the ratio equal or more than "moderate damage" (R^*_m) were evaluated for the areas using the local government data.

The evaluated damage ratios by the local government damage criteria must be then converted to those by the AIJ & CPIJ's survey (the BRI data). Since we have both sets of data for Ashiya City, the damage ratios for the city were employed to prepare the relations for the conversion. The damage rations of low-storied wood-frame buildings for all the blocks by the BRI data in Ashiya City were compared to those obtained from the survey by the city government for the purpose of property tax reduction.

Figure 3 compares the damage ratios from the two data sets: (a) R_h and R^*_h, (b) R_m and R^*_h, and (c) R_l and R^*_m. It can be seen in the figure that R_h is roughly half of R^*_h in the range up to 20%, and that the equality can be almost observed in the relationships (b) and (c) as follows:

$$R_h = R^*_h / 2 \tag{1}$$

$$R_m = R^*_h \tag{2}$$

$$R_l = R^*_m \tag{3}$$

Using these relations, the damage ratios compatible with BRI data were estimated for the regions without BRI data.

Table 1 shows that strong ground motion indices observed by the seismometers used in this study and the damage ratios of residential buildings near the seismometers. Note that the strong ground motion indices used in this study are the larger of the two horizontal components (Ansary et al., 1995).

Fragility Curves of Residential Buildings

The fragility curves of wood-frame buildings were constructed using the relationship between the damage ratio of low-storied residential buildings and the strong motion indices in the Kobe Earthquake. For a strong motion value x, the cumulative probability $P_R(x)$ of the occurrence of the damage equal or higher than rank R is assumed to be log-normal (normal for the JMA intensity) as follows:

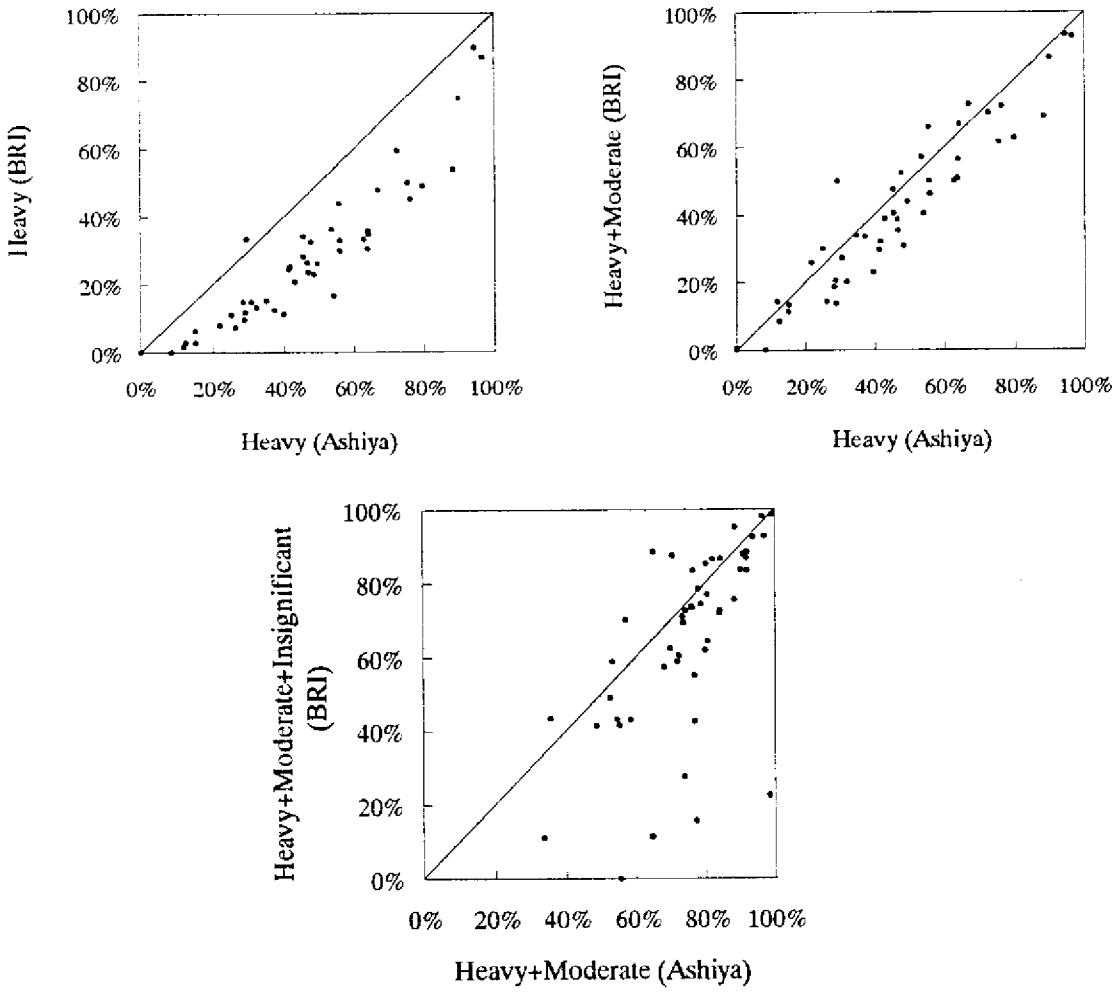

Fig. 3 Comparison of damage ratios for two damage investigations in each district block of Ashiya City

$$P_R(PGA) = \Phi((\ln PGA - \lambda)/\zeta) \tag{4}$$

$$P_R(PGV) = \Phi((\ln PGV - \lambda)/\zeta) \tag{5}$$

$$P_R(SI) = \Phi((\ln SI - \lambda)/\zeta) \tag{6}$$

$$P_R(I) = \Phi((I - \lambda)/\zeta) \tag{7}$$

in which Φ is the standard normal distribution and λ and ζ are the mean and the standard deviation of *ln PGA*, *ln PGV*, *ln SI* and *I*. The two parameters of the distributions, λ and ζ, were determined by the least square method on the log-normal probability paper shown as Fig. 4. Table 2 summarizes the results of the regression for each strong ground motion index. Figure 5 shows the fragility curves for low-storied residential buildings in Japan for PGA, PGV, SI and JMA intensity based on the building damage data due to the Kobe Earthquake.

Table 1 Site of seismometers, their records and the damage ratios of residential buildings near the seismometers

	Observation Point	PGA (gal)	PGV (cm/s)	SI (cm/s)	Intensity	Total Number (Residential)	R_h (%)	R_m (%)	R_l (%)
AMH	Amagasaki Harbor	507	56	63	5.7	442	0.714	5.95	26.9
AMK	Amagasaki Viaduct	294	49	56	5.7	496	3.33	4.76	25.0
AMT	Taketani Elementary School	321	50	58	5.7	939	1.49	11.0	49.8
SGK	Research Institute of Kansai Electric Power	652	49	72	6	1,407	0.273	9.27	45.1
TKT	JR Takatori Station	655	119	139	6.5	660	57.4	85.7	95.3
FUK	Fukiai Gas Supply Station	806	119	150	6.5	122	17.7	25.7	48.7
JMA	JMA Kobe Station	818	91	115	6.4	308	5.79	18.5	71.0
KOB	Motoyama No.1 Elementary School	770	78	74	6.1	641	18.4	33.4	63.9
TKZ	JR Takarazuka Station	685	85	92	6.2	416	11.6	21.3	42.8
JR Shin-Osaka	JR Shin-Osaka Station	216	41	48	-	22,696	0	0	6.17E-02
Yoshino	Yoshino Elementary School	211	31	37	5.4	14,505	4.14E-03	1.38E-02	0.834
JMA Osaka	JMA Osaka Station	81	19	16	4.5	17,232	0	0	5.80E-03
Yotsubashi	Yotsubashi Bridge	270	30	27	5.1	16,153	5.57E-03	1.86E-02	8.05E-02
Iwasaki	Iwasaki Gas Supply Station	172	24	29	5.1	16,153	5.57E-03	1.86E-02	8.05E-02
Senri	Senri Gas Supply Station	299	29	37	5.4	72,288	4.15E-03	1.38E-02	0.44
JR Shin-Takatsuki	JR Shin-Takatsuki Substation	297	-	-	-	69,063	0	0	1.74E-02
Morikawachi	Morikawachi Elementary School	212	27	33	5.3	112,557	1.33E-03	4.44E-03	1.51E-02

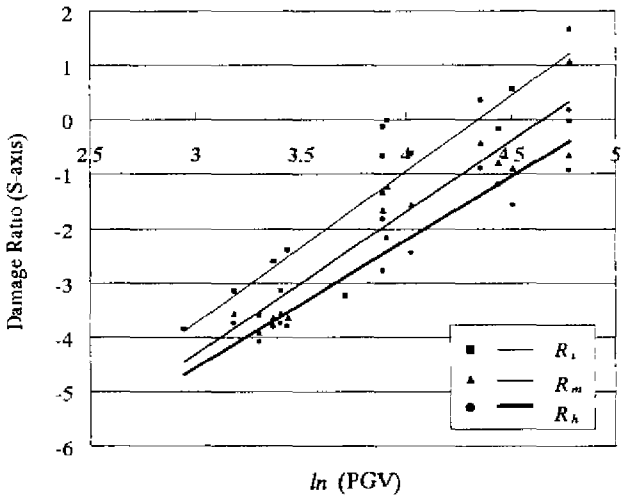

Fig. 4 Relationship between PGV and damage ratio of residential buildings plotted on log-normal probability paper

Table 2 Parameters of fragility curves for residential buildings based on the BRI data

Rank	PGA (cm/s^2)			PGV (cm/s)			SI (cm/s)			JMA Intensity		
	λ	ζ	R^2	λ	ζ	R^2	λ	ζ	R^2	λ	ζ	R^2
R_h	7.23	0.511	0.659	4.95	0.429	0.912	5.18	0.461	0.827	6.74	0.403	0.821
R_m	6.82	0.429	0.722	4.65	0.382	0.885	4.84	0.400	0.844	6.44	0.351	0.835
R_l	6.50	0.431	0.719	4.34	0.358	0.826	4.52	0.392	0.810	6.14	0.361	0.843

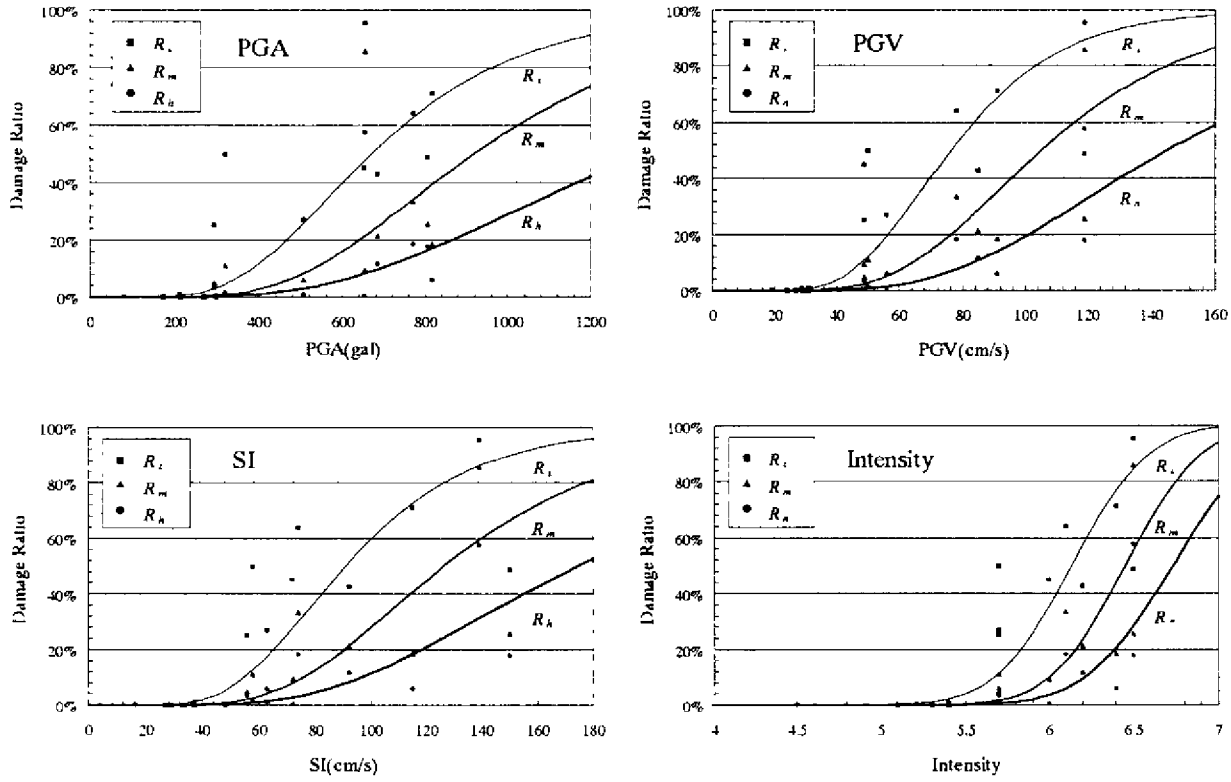

Fig. 5 Fragility curves for residential buildings based on the BRI data

Comparison with Other Researches

Hayashi et al. (1997a,b) constructed the fragility curves for PGV with respect to the use and the number of stories of buildings using the BRI's building damage data and the estimated PGV distribution obtained by a two-dimensional earthquake response analysis. Figure 6 compares the fragility curves for residential buildings by Hayashi et al. and by the authors. It is seen in Fig 6 that, for small PGV values, Hayashi's curves show higher damage probability than ours, and for large PGV values, our relations show higher damage probability. This difference may be resulted from the fact that the data from slightly damaged areas such as Osaka City were considered in this study while not in the Hayashi's study. The difference in the estimation of strong ground motion by the two studies may also be responsible for the difference in the fragility curves: Hayashi estimated the ground motion distribution from the results of the response analysis for the north-south section of Sannomiya area in Kobe while we used the observed ground motions and the building damage data near the seismometers.

ESTIMATION OF GROUND MOTION DISTRIBUTIONS IN THE 1995 KOBE EARTHQUAKE

The fragility curves for the low-storied residential buildings were constructed at the three damage levels. Using these fragility curves and the building damage data compiled by BRI, the ground motion

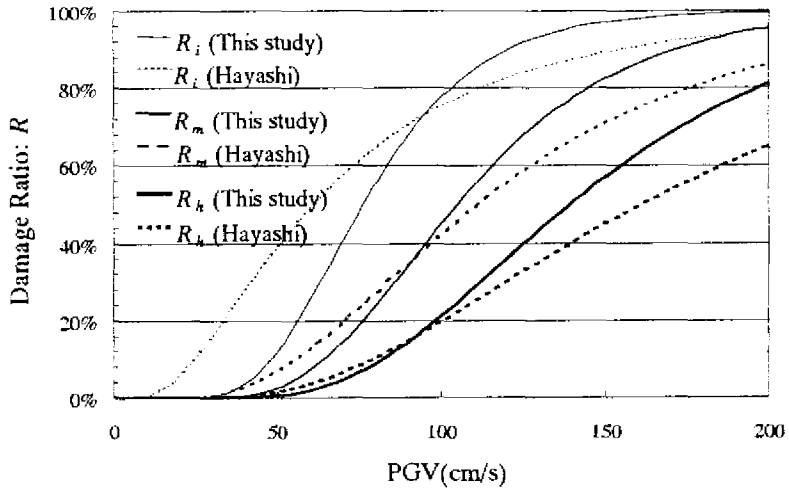

Fig. 6 Comparison of the obtained fragility curves with those by Miyakoshi and Hayashi et al. (1998)

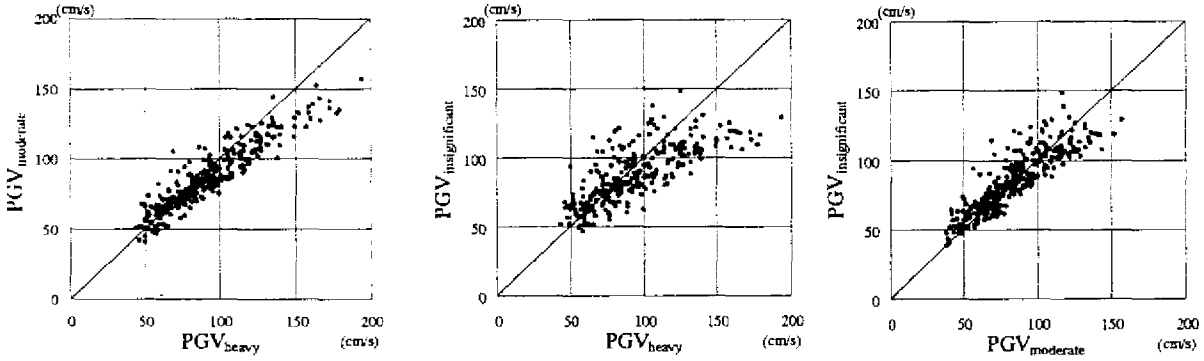

Fig. 7 Comparison of three PGV values estimated from the different damage levels of residential buildings in Nishinomiya City

distributions in the Hanshin area during the Kobe Earthquake were estimated. Since the fragility curves were constructed for low-storied residential buildings, the corresponding building damage data were used in back-calculating strong ground motion distributions.

First, R_h, R_m and R_i were calculated for all the district blocks in the data set. If the number of buildings in a block was less than 10, the strong motion indices were not estimated for such blocks because the sample size is too small to calculate damage ratios. Note that the buildings suffered from fire or uninvestigated were subtracted from the total number. Since the district blocks in Kobe City are small, some of them were combined when calculating damage ratios.

Using the damage ratios calculated by the method mentioned above, three values of a strong motion index corresponding to the three damage levels were obtained by $x_h = P_R^{-1}(R_h)$, $x_m = P_R^{-1}(R_m)$ and $x_i = P_R^{-1}(R_i)$. The three estimated values for PGV were compared in Fig. 7 for Nishinomiya City. In the figure, it is observed that x_h and x_m are almost the same, x_m and x_i are nearly

Table 3 Comparison of observed and estimated ground motion indices for the 17 sites

	Observation Point	Observed Ground Motion Indices				Estimated Ground Motion Indices			
		PGA (gal)	PGV (cm/s)	SI (cm/s)	I	PGA (gal)	PGV (cm/s)	SI (cm/s)	I
AMH	Amagasaki Harbor	507	56	63	5.7	457	56	61	5.8
AMK	Amagasaki Viaduct	294	49	56	5.7	451	55	64	5.8
AMT	Taketani Elementary School	321	50	58	5.7	572	67	76	6.0
SGK	Research Institute of Kansai Electric Power Co.	652	49	72	6.0	414	51	59	5.8
TKT	JR Takatori Station	655	119	139	6.5	1284	135	165	6.7
FUK	Fukiai Gas Supply Station	806	119	150	6.5	611	71	84	6.1
JMA	JMA Kobe	818	91	115	6.4	811	91	109	6.3
KOB	Motoyama No 1 Elementary School	770	78	74	6.1	658	76	90	6.1
TKZ	JR Takarazuka Station	685	85	92	6.2	673	78	92	6.2

equal, and that the relationship between x_h and x_i shows rather large variability. These tendencies were also seen for the other indices and for the data sets of other cities. From these observations, the following rules were adopted to determine single value from the three values:

- If $R_m = 0$, x_i is used.
- If $R_h = 0$ and $R_m \neq 0$, the average of x_m and x_i is used.
- If $R_h \neq 0$, the average of x_h and x_m is used.

Figures 8 and 9 show the distribution of PGV and JMA intensity, respectively, in the Kobe Earthquake obtained by this method. The area of JMA intensity 7 in Fig 9 almost corresponds to the belt of JMA intensity 7 (Fig. 10) determined by JMA's field survey (JMA, 1997). In some areas such as along the seashore, the earthquake ground motion was not estimated due to the shortage of the BRI's residential building data. It is necessary to estimate the ground motion in these areas based on observed records around the areas or using the non-residential building damage data. It is noted that liquefaction occurred in the reclaimed land made the application of the fragility curves more difficult.

Table 3 compares the estimated ground motion indices and the observed ones. The estimated indices almost correspond to the observed ones except for JR Takatori station (TKT) and Fukiai gas supply station (FUK). The difference between the estimation and the observation was large at these two locations, probably due to the regional difference in building characteristics. Note that in our back-calculation method, the low-storied residential buildings were assumed to have similar fragility characteristics in all the studied area. Among the four indices, PGA showed the largest variability in the comparison between the estimated and observed values This observation may be explained by the fact that PGA is strongly affected by high frequency contents of earthquake motion, which have large spatial variability.

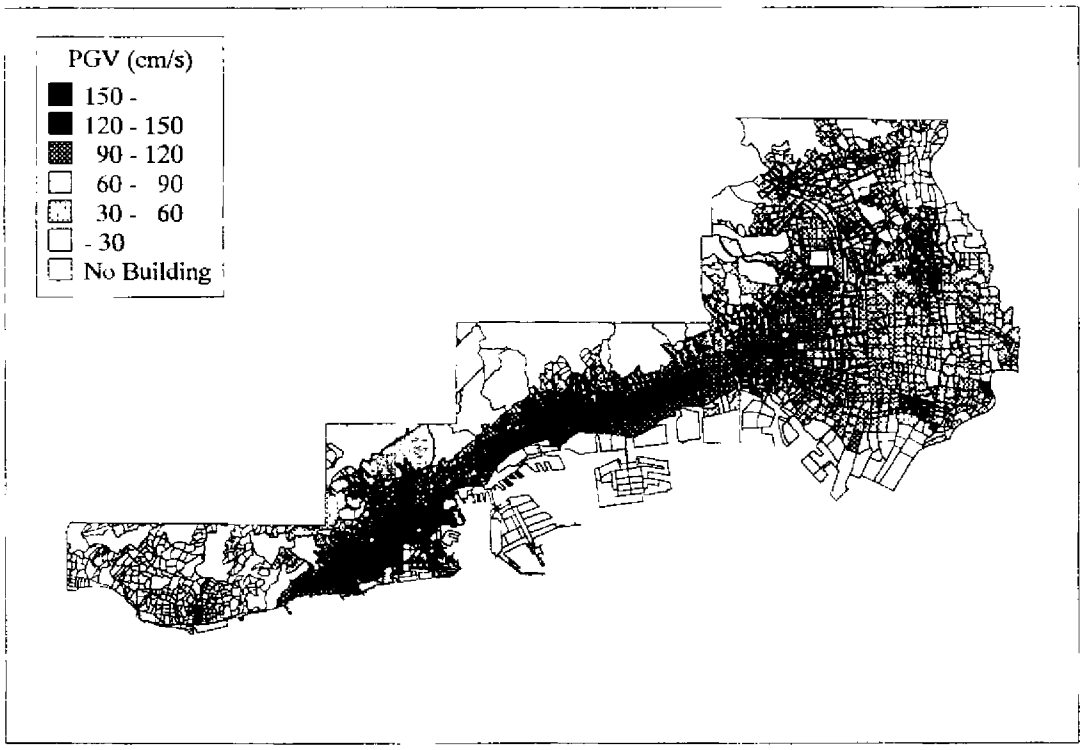

Fig. 8 Distribution of peak ground velocity estimated from the damage ratios of residential buildings

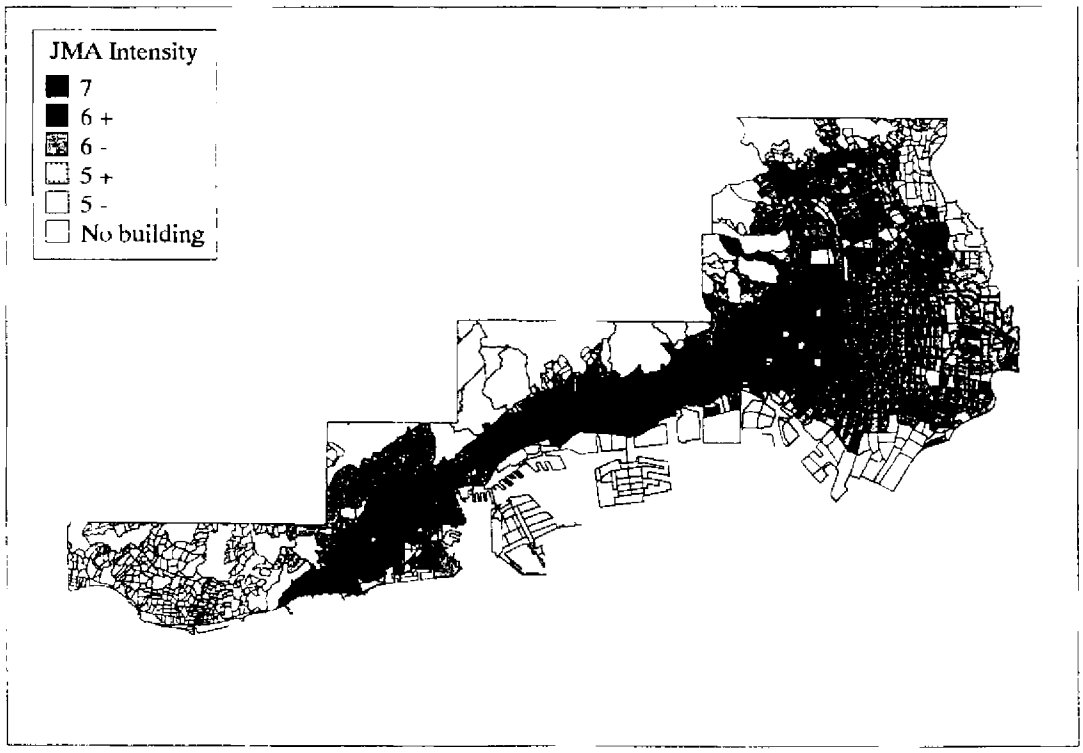

Fig. 9 Distribution of JMA Intensity estimated from the damage ratios of residential buildings

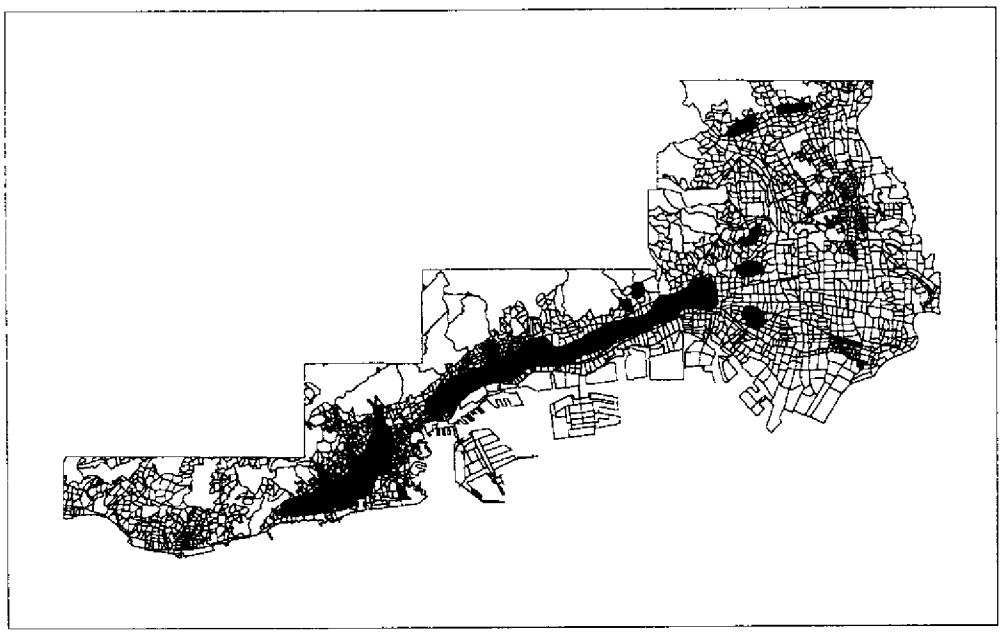

Fig. 10 Belt of JMA Intensity 7 determined by JMA [JMA, 1997]

CONCLUSIONS

In order to evaluate the damage of structures due to an earthquake, it is necessary to estimate ground motion distributions in the stricken area. In the 1995 Kobe Earthquake, however, the number of strong motion records was not large enough to estimate the spatial distribution of ground motion. Hence, the building damage data obtained by the same standard throughout the affected area were employed. Comparing the damage ratios for residential buildings and the recorded strong motion indices (PGA, PGV, SI and JMA intensity), the fragility curves for residential buildings were constructed. Using the obtained fragility curves and the building damage ratios in all the district blocks, the spatial distribution of the strong motion indices were back-calculated for the stricken area of the Kobe Earthquake. The estimated distributions of the strong ground motion may be conveniently used in the investigation of the performance of structures due to the earthquake.

REFERENCES

Ansary, M. A., Yamazaki, F., and Katayama, T. (1995). "Statistical Analysis of Peaks and Directivity of Earthquake Ground Motion," *Earthquake Engineering and Structural Dynamics*, 24 (11), 1527-1539.

Architectural Institute of Japan and City Planning Institute of Japan (1995). *Report of Emergency Damage Survey of the 1995 Hyogoken-Nanbu Earthquake.*

Building Research Institute (1996). *Final Report of Damage Survey of the 1995 Hyogoken-Nanbu Earthquake* (in Japanese).

Ejiri, J., Sawada, S., Goto, Y., and Toki, K. (1996). "Peak Ground Motion Characteristics," *Special Issue of Soils and Foundations*, 7-13.

Hayashi, Y., Miyakoshi, J., Tamura, K., and Kawase, H. (1997a) "Peak Ground Velocity Evaluated from Damage Ratio of Low-Rise Buildings during the Hyogo-Ken Nanbu Earthquake of 1995," *Journal of Structural and Construction Engineering*, 494, 59-66 (in Japanese).

Hayashi, Y., Miyakoshi, J., and Tamura, K. (1997b). "Study on the Distribution of Peak Ground Velocity based on Building Damage during the 1995 Hyogo-Ken Nanbu Earthquake," *Journal of Structural and Construction Engineering*, 502, 61-68 (in Japanese).

Japan Meteorological Agency (1997). *Technical Report of the Japan Meteorological Agency, No. 119, Report on the Hyogo-Ken-Nanbu Earthquake, 1995* (in Japanese).

Kagawa, T., Irikura, K., and Yokoi, I. (1996). "Restoring Clipped Records of Near-Field Strong Ground Motion during the 1995 Hyogo-ken Nanbu (Kobe), Japan Earthquake," *Journal of Natural Disaster Science*, 18(1), 43-57.

Midorikawa, S., and Fujimoto, K. (1996). "Isoseismal Map of the Hyogo-ken Nanbu Earthquake in and around Kobe City Estimated from Overturning of Tombstones," *Journal of Structural and Construction Engineering*, 490, 111-118 (in Japanese).

Miyakoshi, J., Hayashi, Y., Tamura, K., and Fukuwa, N. (1998). "Damage Ratio Functions of Buildings using Damage Data of the 1995 Hyogo-Ken Nanbu Earthquake," *Proceedings of the 7th International Conference on Structural Safety and Reliability (ICOSSAR)*, Kyoto, Japan, 349-354.

Murao, O., and Yamazaki, F. (1999). "Comparison of Building Damage Evaluation by Local Governments after the 1995 Hyogoken-Nanbu Earthquake," *Journal of Architecture, Planning and Environmental Engineering*, 515, 187-194 (in Japanese).

Osaka City Fire Department (1996). *Activity Report of Osaka City Fire Department in the Hyogoken-Nanbu Earthquake* (in Japanese).

Osaka Prefecture (1997). *Report of the Hyogoken-Nanbu Earthquake* (in Japanese).

Shinozuka, M., Chang, S. E., Eguchi, R. T., Abrams, D. P., Hwang, H. H. M., and Rose, A. (1997). "Advances in Earthquake Loss Estimation and Application to Memphis, Tennessee," *Earthquake Spectra*, 13(4), 739-758.

Statistics Bureau, Management and Coordination Agency (1995). *1993 Housing Survey of Japan, Volume 3, Results for Prefectures, Part 27, Osaka-fu* (in Japanese).